

# The GlueX Central Drift Chamber

GlueX-doc-744 (version 4)

Curtis A. Meyer  
Carnegie Mellon University

21 February 2007

## Introduction

The GlueX Central Drift Chamber (CDC) will be a 1.75 *m* long chamber that sits at the upstream end of the GlueX solenoid and surrounds the liquid hydrogen target. It will be used to track particles coming from the GlueX target with polar angles between about 6° and 155° with optimal coverage from about 20° to 140°. Tracks going more forward than about 20° will be tracked by both the CDC and the Forward Drift Chamber (FDC) systems. These tracks will need to travel through the downstream end plates of the CDC, so minimizing the material in this plates is extremely desirable.

The use of a straw-tube chamber in this region allows us to accomplish this goal as the straws can easily support the  $\sim 50$  *g* of tension on each of the  $\approx 3350$  anode wires in the chamber. If one were to go with a wire-cage geometry using field wires, one would need to support about 3000 *kg* of tension between the the end plates. Something which would require both thick end plates as well as thick shell material at both the inner and outer radius of the chamber.

In addition to minimizing material, the straw-tube designs also allows for an extremely well defined electric field through which the ionization drifts. This is especially important given the 2.24 *T* magnetic field. With straw-tubes, the time-to-radius relation can be quite accurately computed using programs such as GARFIELD, and is extremely simple to implement in reconstruction. It also minimizes dead areas in the electric fields which are extremely difficult to model and lead to very poor position resolution for

tracks passing near such regions. A situation which is almost impossible to avoid with wire-cage arrangements.

In order to achieve the physics goals of GlueX, the CDC needs to be able to measure perpendicular distances from the wires ( $\sigma_{r\phi}$ ) to an accuracy of  $\approx 150 \mu m$ . It also needs to be able to make some measurements along the length of the wire ( $\sigma_z$ ) to an accuracy of about  $2 mm$  and be able to make  $dE/dx$  measurements that will allow us to separate kaons and pions below  $450 Mev/c$ . The  $\sigma_{r\phi}$  can be obtained in the straw tube arrangement. The  $\sigma_z$  will be achieved by placing about  $\frac{1}{3}$  of the straw tubes at stereo angles of  $\pm 6^\circ$  relative to the straight wires. The  $dE/dx$  will be achieved by reading out the tubes using Flash ADCs (FADCs) and then making path length corrections.

The contents of this report are an assimilation of the best information on the CDC. As such, it should be considered to supersede all previous documentation where the two differ. In particular, there have been some changes in the physical dimensions of the CDC from that given in the last version of the GlueX design report [1].

## The CDC Geometry

The planned design for the CDC is shown schematically in Figure 1. The active region is  $175 cm$  long with a  $0.6 cm$  thick down-stream end plate and a  $0.9 cm$  thick up-stream endplate. At the down-stream end is a  $5 cm$  thick gas plenum which collects the gas from the tubes. At the upstream end a  $10 cm$  thick plenum for distributing gas and then an additional  $10 cm$  of space for electronics. All cables will be taken off the up-stream end of the chamber. The inner and outer radius of the end plates are  $9 cm$  and  $59 cm$  respectively.

Radially, the chamber will consist of 25 layers of straw tubes arranged in rings around the beam line. The straw tubes are  $0.8 cm$  radius aluminized kapton tubes which surround a gold-plated Tungsten wire. Eight of the layers are placed at stereo angles of  $\pm 6^\circ$ . Table 1 shows the number of straws in each layer as well as the radius of each layer. Note that for the stereo layers, the radius at the center of the chamber and that at the endplates are different. This creates an apparent dead space in the chamber volume.

In Figure 2 are shown where the holes for the straw tubes will be drilled in the upstream end plate. The straight wires are shown in black, while the stereo layers are shown in colour. The layout of the chamber and machining instructions are generated by a simple computer code that takes as input the

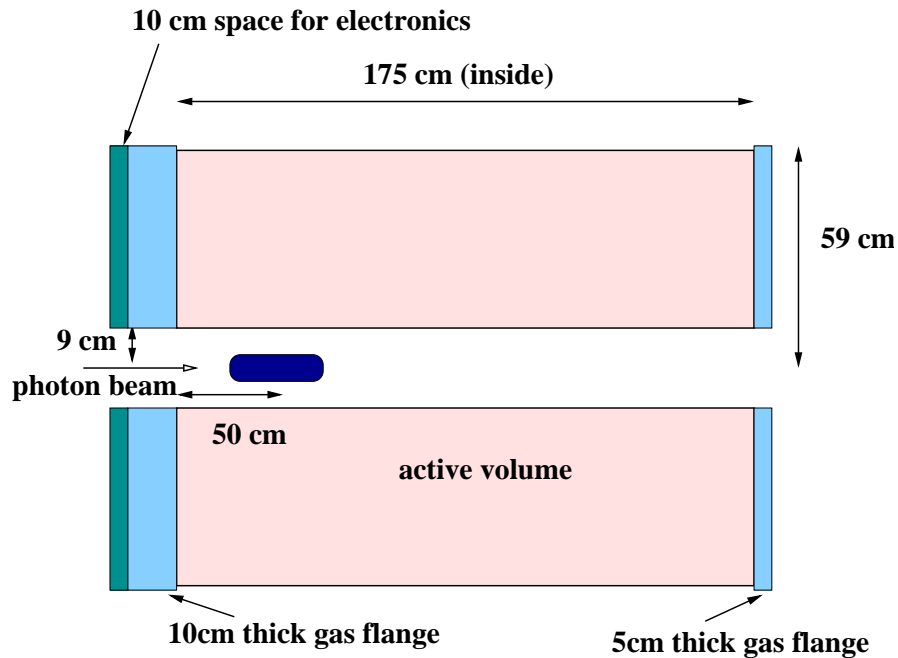


Figure 1: A side view of the CDC. The active region is 175 *cm* long with a 0.6 *cm* thick down-stream end plate and a 0.9 *cm* thick up-stream endplate. At the down-stream end is a 5 *cm* thick gas plenum which collects the gas from the tubes. At the upstream end a 10 *cm* thick plenum for distributing gas and then an additional 10 *cm* of space for electronics. All cables will be taken off the up-stream end of the chamber. The inner and outer radius of the end plates are 9 *cm* and 59 *cm* respectively.

inner and outer radius as well as which layers are stereo. It then lays out the chamber such that all tubes in a given layer are touching each other, and an exact integer number of tubes fit into a layer. The in-layer touching is crucial as the tubes are glued together for structural strength and the integer number eliminates dead spaces as one goes around the beamline.

The wires are held in place by a metallic crimp pin. The pin is inserted in a delrin holder that has holes to allow gas flow. This in turn is inserted into a two-piece donut which is glued into the endplate. For the upstream end, the donuts are made of aluminum to provide an electrical (ground) connection between the endplate and the aluminum on the straw tube. At the downstream end, the donuts are made of Delrin to minimize the material in the

Layer	Wires	Radius (center)	Radius (plate)	Stereo
1	43	10.960	10.960	
2	50	12.741	12.741	
3	57	14.522	14.522	
4	64	16.304	18.718	+6°
5	71	18.086	20.289	+6°
6	78	19.868	21.892	-6°
7	85	21.650	23.522	-6°
8	99	25.214	25.214	
9	106	26.997	26.997	
10	113	28.779	28.779	
11	120	30.561	30.561	
12	127	32.344	32.344	
13	134	34.126	35.343	+6°
14	141	35.908	37.067	+6°
15	148	37.691	38.796	-6°
16	155	39.473	40.530	-6°
17	166	42.274	42.274	
18	173	44.057	44.057	
19	180	45.839	45.839	
20	187	47.621	47.621	
21	194	49.404	49.404	
22	201	51.186	51.186	
23	208	52.969	52.969	
24	215	54.751	54.751	
25	222	56.534	56.534	

Table 1: Shifted in Wire Layout. This has 3337 instrumented wires.

chamber. Figure 3 shows schematically how the straight and stereo layers of tubes are attached to the end plates. In particular, one should note that for the stereo layers, the endplates are machined at a compound angle such that the end of the insert sits flat against the plate. This machining puts a minimum on the thickness of end plate.

An problematic issue that is common with straw-tube chambers is the conductive glue joints that both hold the straws to the feed throughs as well as the feed throughs to the chamber end plates. Careful examination of an

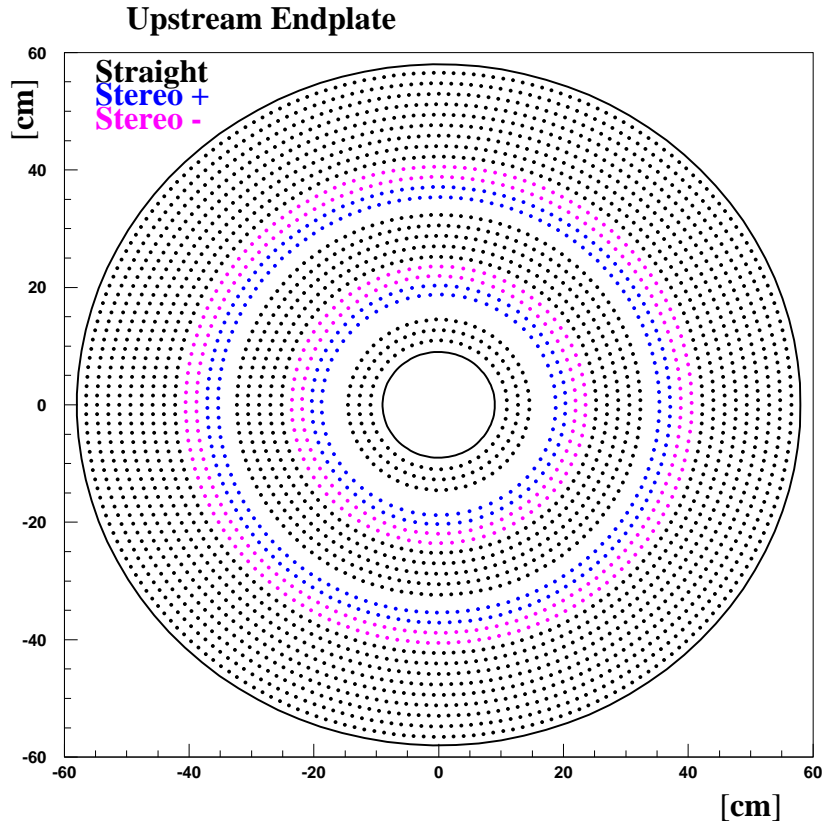


Figure 2: The drill pattern for the up-stream endplate using the 1 geometry. The black dots correspond to straight tubes. The blue dots are the  $+6^\circ$  stereo layers while the magenta is the  $-6^\circ$  stereo layers.

existing straw tube chamber from the Brookhaven EVA experiment showed that all of these joints tend to develop leaks over time. In order to try to alleviate this leak problem, a detailed study of many conducting and non-conducting epoxies was carried out to see if a good glue could be found. The conclusion of this work was that the particular choice of glue did not matter. Instead, the act of inserting one part of a feed through into another part tended to scrape much of the epoxy off the contact surface. This led to a joint with many weak spots that over a short period of time, developed leaks.

Upon careful study of this, it was decided that the only way to guarantee

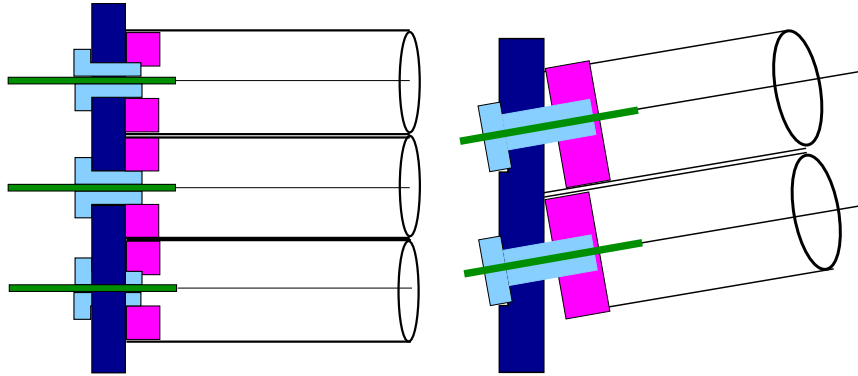


Figure 3: A schematic drawings of the feed throughs for both the normal (**left**) and stereo (**right**) wires in the CDC.

a good glue connection was to develop a system in which one is certain the the glue is actually making solid contact with both surfaces. The result of this is a feed through system as shown in Figure 4. The *donut* is a small tube with a small *glue trough* machined into its perimeter. From one end of the donut, a small *glue port* is drilled from the outside to the *glue trough*. Once the donut has been inserted into the straw tube, a known amount of conducting epoxy can be injected through the *glue port* into the *glue trough*. The strength of the resulting glue joint is solid, independent of the tested epoxies. In fact several test sells have maintained several psi overpressure for nearly nine months without leaking.

Into the donut, it is necessary to glue the insert that both holds the straw tube the chamber end plate and holds the crimp pin. In order to guarantee a good glue joint between the donut and the insert, a small *glue lip* has been machined on the tip of the insert. If a uniform coat of glue is applied to the outside of the *insert*, then when it is inserted into the donut, the epoxy tends to collect in both the *glue lip* and between the *insert* and the chamber end plate. Exactly where we need it to guarantee a good epoxy seal. Using these specially designed feed through systems, we are able to obtain a conducting gas-tight joint with all conducting epoxies that we have tried.

It is these donuts that will be machined out of aluminum for the up-stream end plate and delrin for the down-stream endplate. These parts have been manufactured at Carngie Mellon university for the prototype chamber.

The straw tubes are clearly a crucial element of the design. Work has been done with both aluminized mylar and aluminized kapton tubes. It

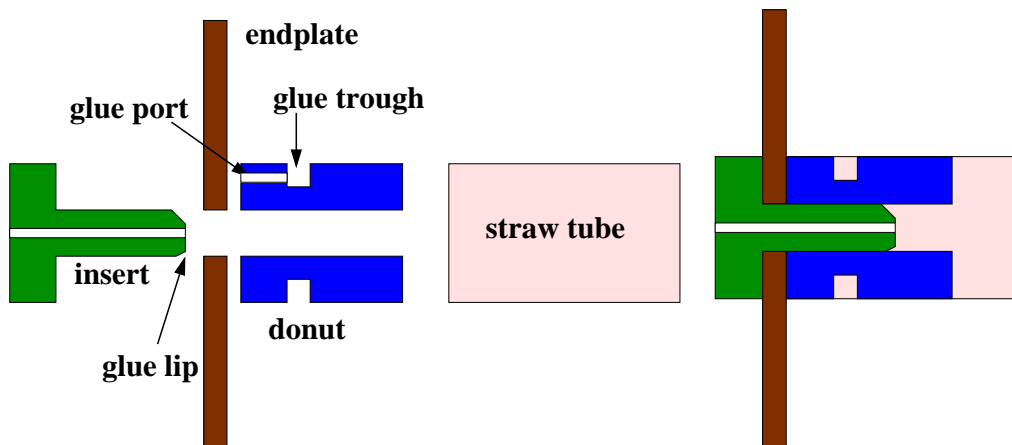


Figure 4: The CMU designed feed throughs which provide a solid glue joint between the straw-tube and the end plate. The left-hand figure shows an expanded view, while the right-hand shows the feed throughs in the chamber end plates.

was found that the mylar tubes were not particularly forgiving during the construction process. Any kink or bump tended to remain in the tube, thus destroying its usefulness. In contrast, the kapton tubes tended to bounce back from just about anything. Once in place, they are much more resilient and significantly less prone to damage. The two main draw backs to kapton are the fact that they are somewhat more expensive than mylar, and that their *springiness* makes them more prone to gravitational sag. Gluing them securely to their neighbor tubes in the final chamber is crucial. However, based on experience with both, it has been decided that kapton tubes will lead to a more resilient chamber, and based on the significantly lower rejection rate (5% versus 95%), will ultimately cost less than mylar.

## The Chamber Gas and the Gas System

The choice of chamber gas plays a significant role in the chamber's performance due to the  $2.24T$  magnetic field. In order to study this, the GARFIELD program [2] has been used to compute electrostatic properties of the straw tubes, both with and without the magnetic field. The results of this work can be summarized in GlueX note 62 [3]. Figure 5 shows an electrostatic calculation for a tube with the wire well-centered in it. Figure 6 shows GARFIELD calculations for two tracks going through a straw tube in three different gas mixtures. The three gas mixtures are Ar(30%)-C<sub>2</sub>H<sub>5</sub>(20%)-CO<sub>2</sub>(50%), Ar(90%)-CO<sub>2</sub>(10%) and Ar(50%)-C<sub>2</sub>H<sub>5</sub>(50%). While in all three cases the time-to-distance relationship is well defined, the longer drift distances of the spiraling tracks introduce a large diffusion contribution to the total resolution. The diffusion resolution,  $\sigma_L$  is also dependent on the gas. Pure argon has an extremely poor resolution, while pure carbon dioxide has a very good resolution. Finally, it is desirable to collect the electrons as quickly as possible. A slow gas, or a very long drift distance can easily push the collection time over a micro second. For this reason, the Argon-Ethane mixture shown in the lower two plots of Figure 6 is an inappropriate mixture. Investigations are ongoing to identify mixtures that will satisfy all of the requirements. To indicate the advantage of good electrostatics, Figure 7 shows what happens to the time-to-distance relation as one goes from zero magnetic field to full magnetic field.

In order to achieve the desired  $150\ \mu m$  resolution in the CDC, we need to account for all possible contributions to the resolution. Table 2 summarizes these. Clearly the most important is the diffusion term, which depends on the gas. In order to achieve this, a gas mixture that contributes about  $120\ \mu m$  for an average  $5\ mm$  drift in a  $\sim 2.5\ kV/cm$  electric field needs to be used. Many gas mixtures satisfy this requirement. The next largest contribution is the gravitational sag. This scales with the length squared, and will go down if the chamber is shorter than  $1.75\ m$ . The timing resolution of  $45\ \mu m$  assumes that the signal is digitized using  $125\ MHz$  flash ADCs and that a timing algorithm that yields times to about  $\frac{1}{3}$  of the digitization are used. Time fitting algorithms that are matched to the pulse shape in chambers usually yield intrinsic time resolutions around 20% of the time bin width.

Currently work is being carried out using a 90% Argon, 10% Carbon-dioxide gas mixture. The gas system currently in use for the prototype will likely evolve into the final system. It consists of an electronic mixer that can



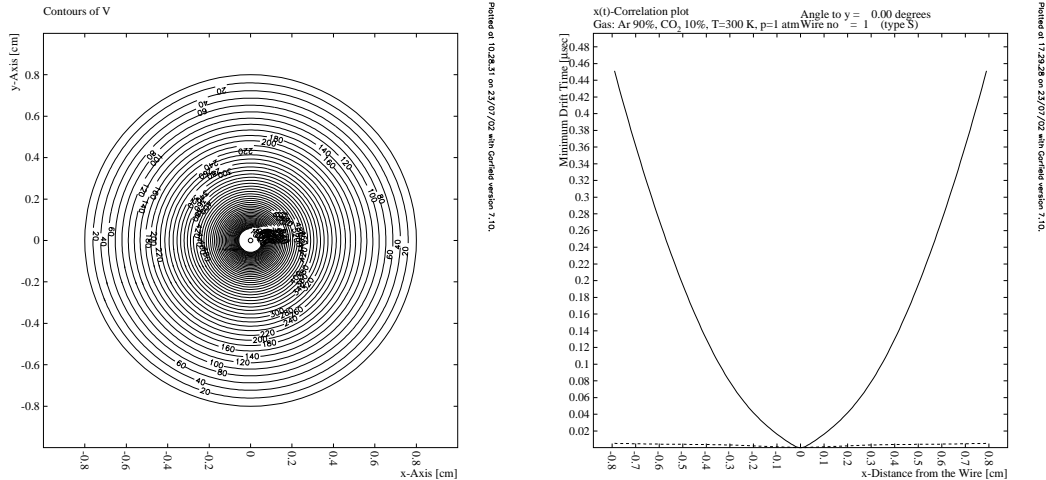


Figure 5: The left-hand plot shows a GARFIELD [2] calculation of the electric field in the straw tube. The right-hand figure shows a typical time-to-distance plot calculated for the straw-tube geometry in the  $2.24 T$  magnetic field.

Effect	Resolution $\mu m$
Diffusion $\sigma_L$	50 to 200 $\mu m$
Geometrical Precision	40 $\mu m$
Gravitational Sag	56 $\mu m$
Electrostatic Deflection	10 $\mu m$
Timing Resolution	45 $\mu m$
Quadrature Total	96 to 216 $\mu m$
Design Resolution	150 $\mu m$

Table 2: The estimated contributions to the ultimate chamber resolution from various known effects. These numbers are based on  $1.75 m$  long,  $20 \mu m$  diameter, Au-W wires under  $50 g$  tension.

handle four gas inputs with individually calibratable controls. The resulting mixture is then pushed into a mixing tank, and then delivered to the chamber. The four input gasses are filtered before entering the system. One of the gas values allows for its output to be bubbled through a chilled liquid such as water or methylal. The current design calls for several gas changes per day in the chamber with the exhaust gas being discarded. Monitors will need

to be installed to monitor the temperature and the oxygen content of the input gas. In addition, a slight over-pressure system will be used to keep the gas pressure slightly above the current atmospheric pressure. Such a system will require monitoring the atmospheric pressure and ultimately correcting the chamber calibrations based on the density of the chamber gas.

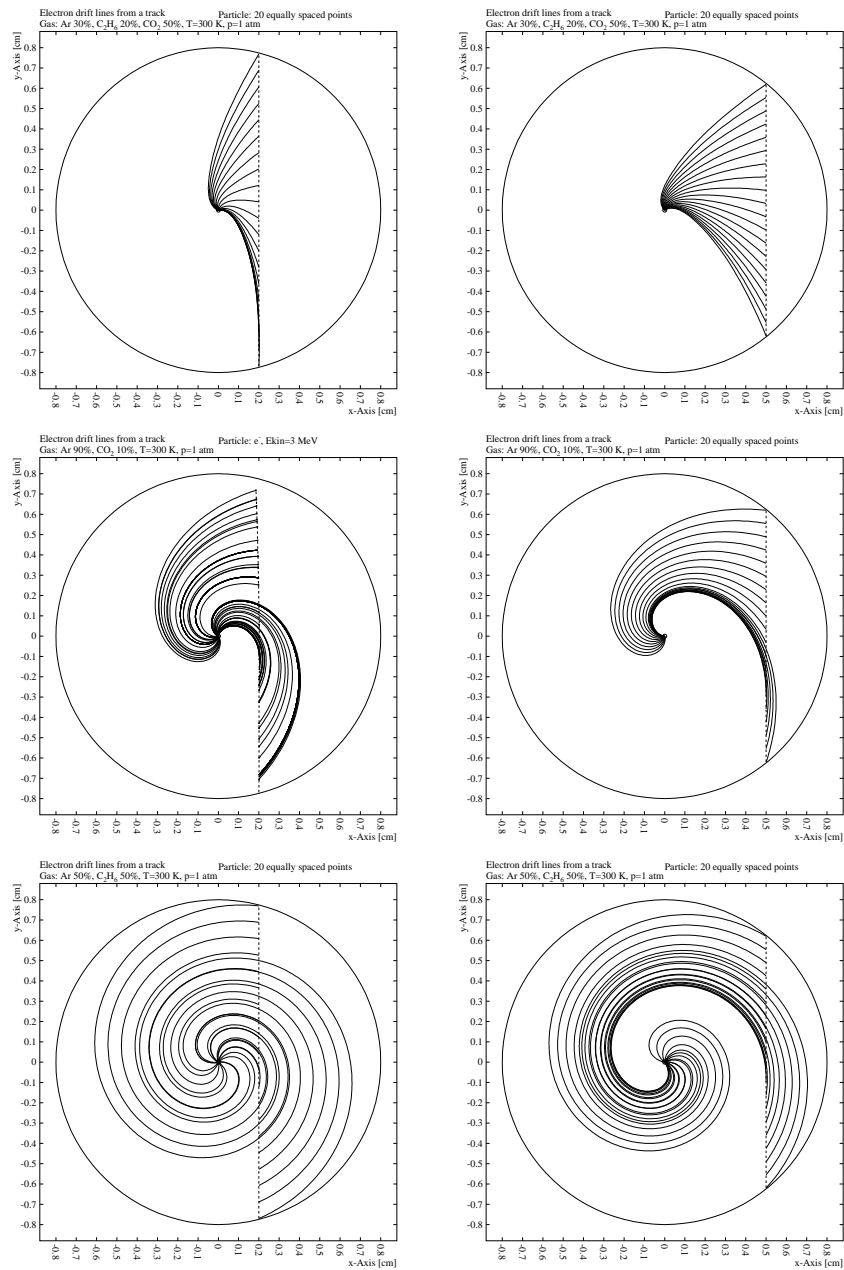


Figure 6: GARFIELD simulations of electrons drifting through a straw tube in the CDC. The curved shape of the tracks is due to the Lorentz angle induced by the 2.25 T magnetic field.

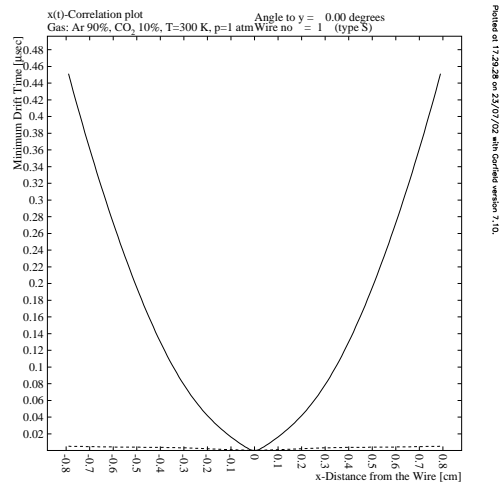
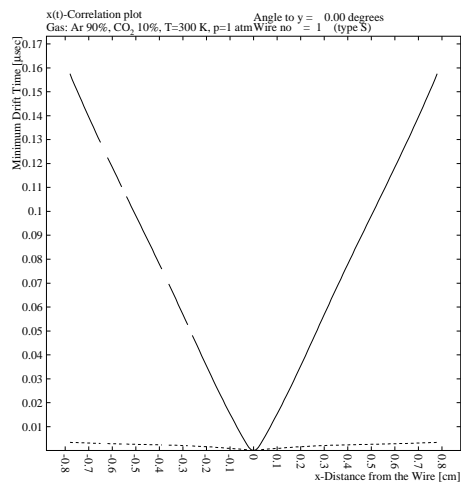


Figure 7: Calculated time versus distance in 90% Argon, 10% Carbon Dioxide mixture. **left**: No magnetic field, **right**: full magnetic field.

## Background Rates in the CDC

Electromagnetic interactions of the beam with the target and other material produce the dominant source of backgrounds in the GlueX detector. It is important to understand what these rates are in the CDC. This will likely limit how close the detector can be to the beamline, as well as the lifetime of the chamber. A detailed study using the Hall-D GEANT (HDGEANT) package has been carried out to calculate the rates in an individual straw tube. For purposes of the study, the tubes were placed at the positions given in Table 1. However, we also added a layer of straw tubes at a radius of  $6.12\text{ cm}$  and another one at  $8.15\text{ cm}$ . These added layers will give us some feel as to how fast the background rates are rising. The rates were estimated by effectively counting the number of background particles over the entire length of a straw tube in each of the layers. For a primary tagged photon flux of  $10^8\text{ }\gamma/s$ , the measured rates as a function of layer are shown in Figure 8.

The results for the innermost four layers (yellow in Figure 8 are summarized in Table 3. The planned CDC has its innermost strawtubes at a radius of about  $10.5\text{ cm}$ , which would lead to an estimated  $\approx 40\text{ KHz}$  rate at the highest GlueX beam fluxes. While it also appears that it might be possible to move the innermost layers closer to the beam line, perhaps down to about  $6\text{ cm}$ , the added material closer to the beam line is likely to degrade the performance of the rest of the detector. If it were desirable to make such a change, an overall optimization of the detector would need to be done with the new geometry. Such a change would also preclude the addition of a future near-target detector which might well be desirable as a future upgrade to GlueX.

Radius	Rate
$6.12\text{ cm}$	$100\text{ KHz}$
$8.15\text{ cm}$	$59\text{ KHz}$
$10.19\text{ cm}$	$41\text{ KHz}$
$12.02\text{ cm}$	$33\text{ KHz}$

Table 3: The computed background rates for strawtubes placed at several different radii around the beam. The planned innermost tubes are at about  $10.5\text{ cm}$  radius.

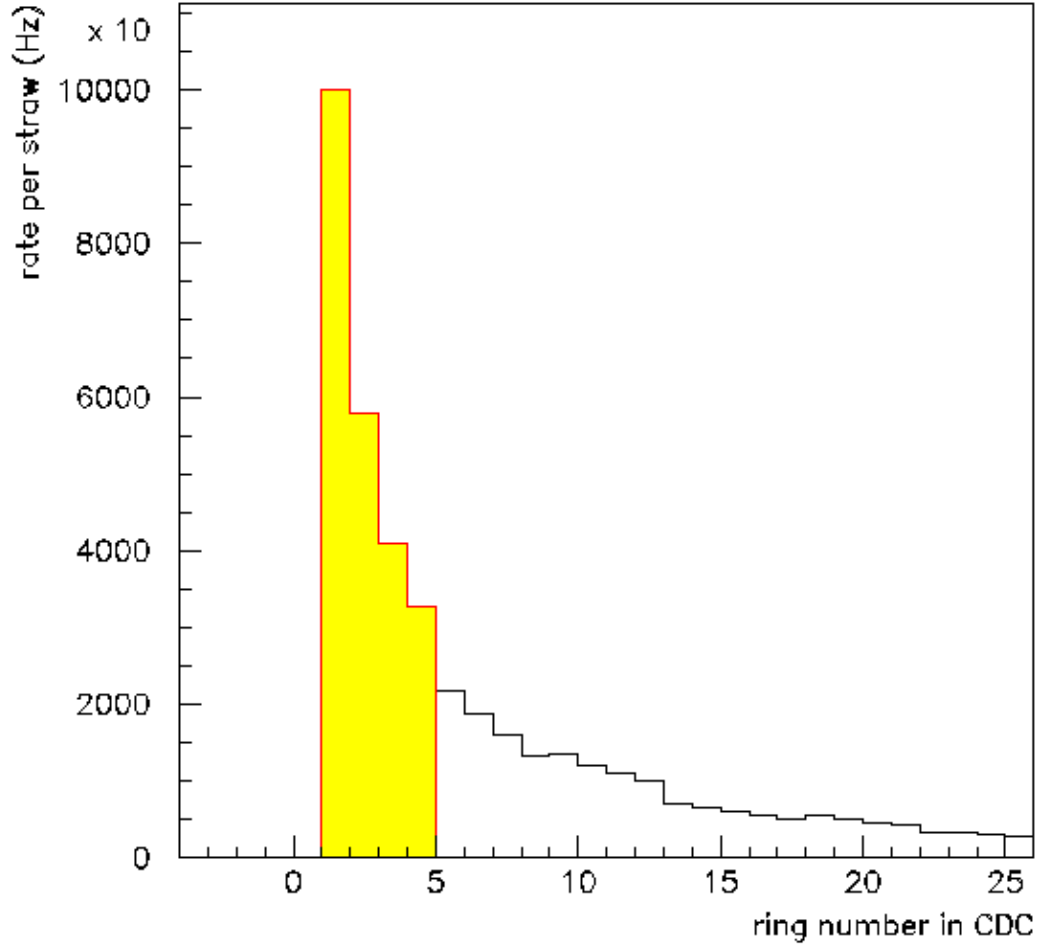


Figure 8: The electromagnetic background rates as a function of layer in the CDC for  $10^8$  tagged photons per second. The rates are per tube with the innermost four tubes placed at  $6.12\text{ cm}$ ,  $8.15\text{ cm}$ ,  $10.19\text{ cm}$  and  $12.02\text{ cm}$  respectively (shown in yellow in). Even at a  $6\text{ cm}$  from the target, the background rate is only  $100\text{ KHz}$  for the highest photon fluxes.

## Vertex Resolution

The ability to reconstruct the primary, and possible secondary vertices is an important consideration in GlueX. The CDC is the tracking detector closest to the target, and is therefore the main component involved in vertex reconstruction. Nominally, the closer the measurements are to the beam line, the better the vertex measurement will be. The further one has to project tracks through the magnetic field, the worse things will be. Similarly, for measuring the  $z$ -coordinate of the vertex, the radius of the stereo layers in the CDC play a similar role. Simple arguments would advocate moving the first set of stereo layers as close to the beam line as possible to try and match the  $x$ - $y$  to the  $z$  resolution. Unfortunately, for the stereo layers to provide optimal information, the tracks need to be well mapped (with straight layers) on both the inner and outer sides of the stereo layers. This leads to the configuration in Table 1 where the innermost three layers are straight.

A detailed study of the vertex resolution as a function of where the straight and stereo layers are placed was carried out and is described in GlueX note 388 [4]. The results of this study are summarized in Figure 9 where we plot the vertex resolution as a function of the radius of the innermost layer. The layer placement given in Table 1 will lead to a vertex resolution of  $\sigma_{xy} \approx 0.5 \text{ mm}$  and  $\sigma_z \approx 4 \text{ mm}$ . It is also seen that assuming that one could move the stereo layers into  $6 \text{ cm}$  would only improve  $\sigma_z$  to about  $3 \text{ mm}$ .

## Chamber Electronics

A straw tube chamber has the anode wires held at positive high voltage and the surface of the straws held at ground. Electrons drift to the anodes where they undergo gas amplification and ultimately yield an electronic pulse on the wire. Because both the high voltage and the signal are on the same wire, a special high-voltage distribution board needs to be built that capacitively couples the anodes to the preamplifiers.

Based on early experience with what were effectively antennas, and subsequent discussions with people from the CLEO collaboration, we developed a design for the High-voltage Distribution Board. In close consultation with Gerard Visar of Indiana, we refined this design on a CAD system and eventually had several boards produced. These boards were designed to have the

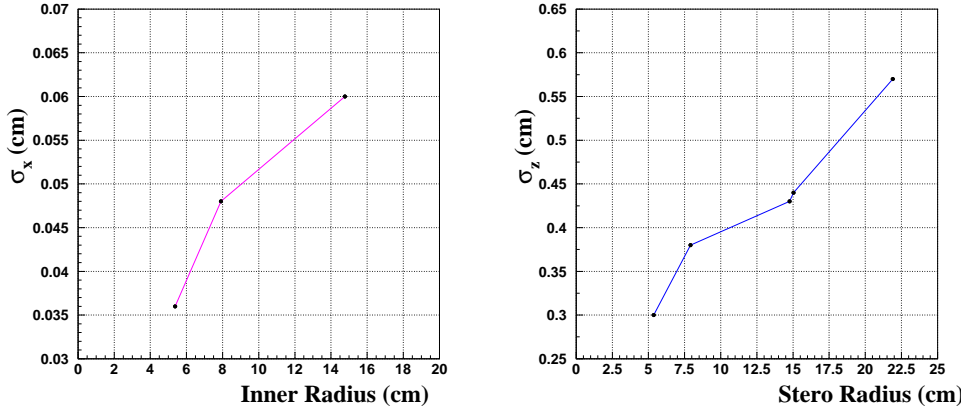


Figure 9: The estimated vertex resolution as a function of the radius of the innermost layer of tubes. For the case of the  $x$  resolution, this corresponds to the straight layers. For the  $z$  resolution, it is a function of the location of the first stereo layer.

electronic layout of the final boards and their performance to date indicates that this is likely to be true. However, the exact shape, size and connector types for the final boards awaits the design of the chamber preamplifiers. The cross-talk has been significantly reduced and with a preamplifier plugged directly into the distribution boards, the signal to noise appears to be a very reasonable level in the lab. Figure 10 shows a photo of the current version of the high-voltage board with a CLAS preamplifier mounted on it. The High-voltage Distribution Board (HVDB) will mount on the outside of the upstream gas plenum, and shielded wires will pass through the plenum and connect to the anodes.

The chamber preamplifiers will be common with the FDC system and are currently being prototyped by members of the GlueX collaboration in Alberta and the University of Pennsylvania. The final preamplifier will mount directly on the HVDB and then drive a 24-pair cable that will connect into to a shaper board designed by Gerard Vissar at Indiana. This will then feed into a Flash ADC (FADC) system running at a rate of at least  $100\text{ MHz}$ . The same electronic chains will be used for both the CDC and the FDC and the ultimate clock rate on the FADC will be determined by prototype work currently being carried out.



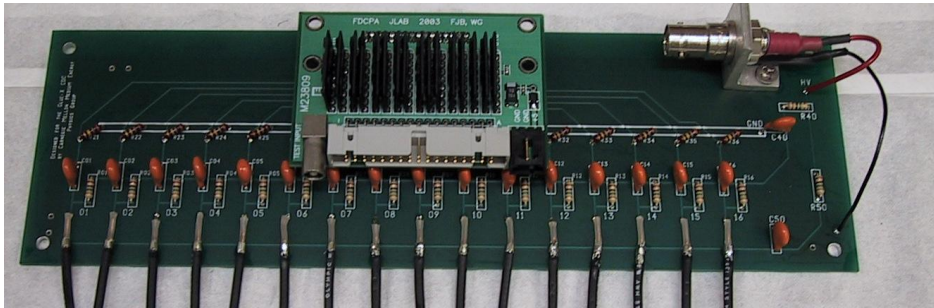


Figure 10: The prototype high-voltage distribution board with a CLAS preamplifier card mounted directly on the board.

## Chamber Installation and Calibration

The CDC will sit on a pair of rails located inside the solenoidal magnet. For installation and extraction of the chamber, the rails will *mate* with external rails mounted to a cart on the upstream side of the detector. The CDC will be able to be inserted and extracted with its cabling intact. Positioning of the chamber will include fiducial marks that can be surveyed as well as possible positioning pins. The final such system still needs to be designed. However, it is crucial that the relative position of the CDC and the FDC be accurately known in order to achieve that ultimate resolution. In addition, for regions where the magnetic field is not uniform, it will be necessary to know the absolute locations of the chambers with reasonable accuracy.

For calibration of the chambers, there will be a system that allows us to send pulses down to the inputs of the preamplifiers. This will allow for a relative timing measurement of each channel as well as a method to monitor gain variation in individual channels. As noted earlier, it will also be necessary to monitor the gas pressure and temperature and then make corrections for density changes in the gas.

The starting point of the reconstruction will be a time-to-radius relation that can be accurately calculated using the GARFIELD program. With this as a starting point, we anticipate being able to select a reasonable profuse reaction that can be reconstructed and then used to fine tune the calibrations.

# 1 Chamber Maintenance

The CDC is designed such that all the electronics is on the up-stream end of the chamber. These will be accessible without removing the chamber from the magnet. In the case where a wire were to break and short out against the side of the strawtube, we anticipate that the High Voltage will be distributed in blocks such that some section of the chamber could be turned off. It is also possible from the upstream end to disconnect the high voltage from a single wire, though the operation of moving things out of the way may well make this one to two shift long operation.

# 2 Charge Division in The Chamber

An alternative method to measure the position along the length of a wire in the straw tube is through charge division. Here, a

## List of Design Parameters

Table 4: Geometry

Active volume inner radius:	10.16 <i>cm</i>
Active volume outer radius:	57.4 <i>cm</i>
Active length:	175 <i>cm</i>
Chamber assembly outer radius:	60.0 <i>cm</i>
Axial layers (1-4):	10.2 to 15.3 <i>cm</i>
Stereo layers (5-8):	15.9 to 22.5 <i>cm</i>
Axial layers (9,13):	24.4 to 33.2 <i>cm</i>
Stereo layers (14-17):	33.4 to 40.3 <i>cm</i>
Axial layers (18,23):	41.5 to 57.4 <i>cm</i>
Thickness per layer (g/cm <sup>2</sup> ):	0.051
Thickness per layer (rad. lengths):	0.0014
Thickness per 25 layers (rad. lengths):	0.035

Table 5: Material

Gas (at 1 at.):	$Ar/CO_2/CH_4$ 80/10/10 (possibly)
Number of cables : (50-conductor shielded ribbon cables)	3337/24
Positioning accuracy of sense wires (x,y):	10 $\mu m$
Positioning accuracy of package (z):	0.5 mm
Thickness of inner shell (g/cm <sup>2</sup> ):	0.162
Thickness of inner shell (rad. lengths):	0.0067
Thickness of outer shell (g/cm <sup>2</sup> ):	1.02 cm of fiberglass
Thickness of outer shell (rad. lengths):	0.031
Strawtube (diameter):	1.6 cm
Strawtube (material):	Aluminized Kapton
Strawtube (thickness):	100(5) $\mu m$ Kapton(Al)
Number of sense wires (20 micron gold-plated W):	3337 $\pm$ 1.5%
Upstream Endplate:	0.9 cm Al
Downstream Endplate:	0.6 cm Al
Upstream Feedthrus:	Al
Downstream Feedthrus:	Delrin
Plenums:	Plexiglas

Table 6: Location active area

Upstream gas plenum:	-3 cm
Upstream active volume:	17 cm
Downstream active volume:	192 cm
Downstream gas plenum:	202 cm

Table 7: dE/dX capability

Sense wires:	YES
Momentum Range:	$p \leq 450 MeV/c$

## Response to the GlueX Detector Review

The original CDC design had an active length of 200 cm and 23 instrumented layers going from about 16 cm to 58 cm radius ( $L = 42$  cm). The wire layout is summarized in Table 11. As indicated in the table, the smallest radius of

Table 8: Operation:

Nominal operating voltage (sense):	+1900 V
Nominal gas gain:	$5 \times 10^4$
Gas flow:	5/day

Table 9: Preamplifier and Readout

Nominal gain:	$5^4$
Noise level:	
Rise time:	$\sim 50$ ns
Tail compensation:	YES
Cable length to post-amp:	30 m
Discriminator output:	NO
Sense wires:	100 MHz FADCs

Table 10: Calibration and Resolution

Sense wires (selected charge):	electronic pulser
Perpendicular to wire ( $\sigma$ ):	150 $\mu$ m
z-position from stereo ( $\sigma$ ):	2 mm
z-position from charge division:	8 cm

a stereo wire is about 23 cm at the center of the chamber.

One of the questions raised at the GlueX detector review had to do with vertex resolution and the placement of the stereo layers. It was suggested that the stereo layers be brought closer to the beam line to improve the z-vertex resolution from tracks. A careful study was carried out on this shortly after the review and concurred that moving both the straight and stereo layers closer to the beam axis would make a significant improvement in vertex resolution.

## References

- [1] The GlueX Collaboration, **The GlueX Detector Review Mini-Design-Report**, GlueX Document 346, October 2004.
- [2] Rob Veenhof, **The GARFIELD Program, Simulation of Gaseous Detectors**, <http://garfield.web.cern.ch/garfield/>, (1984).

Table 11: Reference Wire Layout. This has 3349 instrumented wires.

Layer	Wires	Radius (center)	Radius (plate)	Stereo
1	63	16.049	16.049	
2	70	17.831	17.831	
3	77	19.613	19.613	
4	84	21.395	21.395	
5	91	23.178	25.449	+6°
6	98	24.960	27.082	+6°
7	105	26.742	28.733	-6°
8	112	28.524	30.398	-6°
9	126	32.089	32.089	
10	133	33.871	33.871	
11	140	35.654	35.654	
12	147	37.436	37.436	
13	154	39.218	39.218	
14	161	41.001	42.326	+6°
15	168	42.783	44.055	+6°
16	175	44.566	45.788	-6°
17	182	46.348	47.525	-6°
18	193	49.149	49.149	
19	200	50.932	50.932	
20	207	52.714	52.714	
21	214	54.497	54.497	
22	221	56.279	56.279	
23	228	58.062	58.062	

- [3] Zebulun Krahn and Curtis A. Meyer, **Gas Composition Study for the Straw Tube Chamber in the GlueX Detector at Jefferson Lab**, GlueX Document 62, November 2002.
- [4] Curtis A. Meyer, **A Study of Vertex Resolution in GlueX**, GlueX Document 388, November 2004.